JOURNAL OF APPLIED PHYSICS VOLUME 90, NUMBER 3 1 AUGUST 2001

Influence of surface processing and passivation on carrier concentrations and transport properties in AlGaN/GaN heterostructures

X. Z. Dang and E. T. Yu[a)]
Department of Electrical and Computer Engineering, University of California at San Diego, La Jolla, California 92093-0407

E. J. Piner and B. T. McDermott
ATMI/Epitronics, 21002 North 19th Avenue, Suite 5, Phoenix, Arizona 85027-2726

(Received 19 February 2001; accepted for publication 2 May 2001)

The influence of surface chemical treatments and of deposition of a SiO_2 surface passivation layer on carrier distributions and mobility in $Al_xGa_{1-x}N/GaN$ heterostructure field-effect-transistor epitaxial layer structures is investigated. Surface chemical treatments are found to exert little influence on carrier distribution and mobility. Deposition of a SiO_2 surface passivation layer is found to induce an increase in electron concentration in the transistor channel and a decrease in mobility. These changes are largely reversed upon removal of the SiO_2 layer by wet etching. These observations are quantitatively consistent with a shift in Fermi level at the $Al_xGa_{1-x}N$ surface of approximately 1 eV upon deposition of SiO_2, indicating that the $Al_xGa_{1-x}N/SiO_2$ interface has a different, and possibly much lower, density of electronic states compared to the $Al_xGa_{1-x}N$ free surface. © *2001 American Institute of Physics.* [DOI: 10.1063/1.1383014]

I. INTRODUCTION

$Al_xGa_{1-x}N/GaN$ heterostructure field-effect transistors (HFETs) are currently of outstanding interest for application in high-power microwave-frequency electronic systems. Although very impressive device performance has been achieved by a number of groups,[1–5] pronounced current slump effects,[6–8] variations in device response under pulsed and variable-frequency bias conditions,[9–11] and microwave power degradation[1,9] are often observed. A variety of phenomena, including surface, interface, and bulk trap states[6–8,12] and dielectric response,[11] have been invoked to explain these effects. Surface passivation using silicon nitride has recently been found to mitigate current slump and microwave power degradation,[13] but a much improved understanding of these phenomena and their physical origins will be required to design, fabricate, and optimize the performance of nitride HFET structures for microwave power applications.

In this article, we describe characterization of carrier distributions and charge transport in $Al_xGa_{1-x}N/GaN$ HFET epitaxial layer structures subjected to various surface treatments and passivated by deposition of SiO_2. Our results indicate that deposition of SiO_2 on an $Al_xGa_{1-x}N/GaN$ HFET epitaxial layer structure induces substantial, reversible changes in carrier distribution consistent with a large shift in the position of the Fermi level at the $Al_xGa_{1-x}N/SiO_2$ interface compared to that at the $Al_xGa_{1-x}N$ surface; our observations indicate that a substantial change, possibly a large reduction, in the electronic density of states at the $Al_xGa_{1-x}N/SiO_2$ interface occurs compared to that at a free $Al_xGa_{1-x}N$ surface. These results are of relevance for approaches to mitigation of current slump effects based on dielectric passivation layers, surface passivation for other nitride-based device structures,[14] and metal–insulator–nitride semiconductor HFET structures in which a dielectric layer such as SiO_2 is incorporated within the transistor gate structure to reduce gate leakage current.[15–17]

II. EXPERIMENT

The $Al_xGa_{1-x}N/GaN$ HFET epitaxial layer structures used in these studies were grown by metalorganic chemical vapor deposition on sapphire substrates. Structures with either intentionally doped or nominally undoped $Al_xGa_{1-x}N$ barrier layers were employed. The doped-barrier sample, shown schematically in Fig. 1(a), consisted of a 3 μm nominally undoped GaN buffer layer followed by a 20 Å $Al_{0.25}Ga_{0.75}N$ spacer layer, 150 Å $Al_{0.25}Ga_{0.75}N$ doped with Si at a concentration of $8\times10^{18}\,cm^{-3}$, and finally, 30 Å undoped $Al_{0.25}Ga_{0.75}N$. The undoped-barrier sample, shown schematically in Fig. 1(b), consisted of a 3 μm nominally undoped GaN buffer layer followed by a 200 Å nominally undoped $Al_{0.30}Ga_{0.30}N$ barrier layer. Van der Pauw patterns were fabricated on these samples using Al/Ti to form ohmic contacts. Contacts on the undoped-barrier sample were annealed in N_2 at 830 °C; no annealing was required to form low-resistance ohmic contacts to the doped-barrier sample.

Both types of samples were then subjected to a variety of surface treatments, after each of which Hall measurements were performed at room temperature to assess the effect of these treatments on sheet carrier concentration and mobility in the two-dimensional electron gas (2DEG) channel of the $Al_xGa_{1-x}N/GaN$ HFET structures. Specifically, samples were subjected sequentially to rapid thermal annealing at 600 °C in N_2, a 10–15 s etch in $HCl:HF:H_2O$ (1:1:2), a 10 s etch in 14% HF buffered oxide etch (BOE), deposition of a ~1300 Å SiO_2 passivation layer, and subsequent removal of

---

[a)] Electronic mail: ety@ece.ucsd.edu

0021-8979/2001/90(3)/1357/5/$18.00

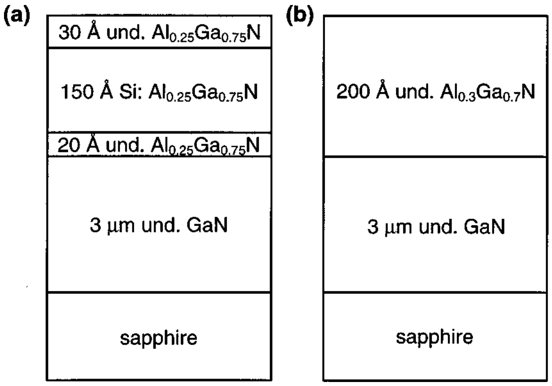

FIG. 1. Schematic diagrams of $Al_xGa_{1-x}N$/GaN HFET structures with (a) doped and (b) undoped $Al_xGa_{1-x}N$ barrier layers.

the passivation layer by etching in 14% HF BOE. The SiO_2 passivation layer was deposited using plasma-enhanced chemical vapor deposition (PECVD) at a substrate temperature of 300 °C and rf power level of 30 W. After each etch step described above, the sample was rinsed in deionized water and blown dry prior to measurement.

III. RESULTS AND DISCUSSION

Figure 2 shows sheet carrier concentration n_s and Hall mobility μ measured after each processing step described above for the doped-barrier sample. As shown in the figure, the sheet carrier concentration is essentially unaffected by annealing at 600 °C and by etching in HCl:HF:H_2O. However, the mobility decreases slightly following each of these steps. Subsequent etching in BOE affects neither the mobility nor the sheet carrier concentration. The most noteworthy observations from Fig. 2 are that PECVD deposition of a SiO_2 layer on the $Al_{0.25}Ga_{0.75}N$ surface results in a significant change in both sheet carrier concentration and mobility, and that these changes are essentially reversed upon removal of the SiO_2 layer by etching in BOE for 150 s. Similar behavior is evident in the undoped-barrier sample, as shown in Fig. 3. The observed changes in 2DEG properties upon deposition of the SiO_2 layer are consistent with prior suggestions that $Al_xGa_{1-x}N$ surface properties are closely coupled to 2DEG properties via polarization effects,[18,19] and the observation that removal of the SiO_2 layer largely reverses these changes confirms that $Al_xGa_{1-x}N$ surface properties, rather than plasma-induced damage incurred during PECVD deposition of the SiO_2 layer, are the relevant factor leading to the observed changes in sheet carrier concentration and mobility. Stress within the $Al_{0.25}Ga_{0.75}N$/GaN heterostructure induced by the presence of the SiO_2 layer is unlikely to be a significant factor, as any change in the piezoelectric sheet charge at the $Al_{0.25}Ga_{0.75}N$/GaN interface due to the $Al_{0.25}Ga_{0.75}N$ piezoelectric polarization field will be compensated by a corresponding change, approximately equal in magnitude and opposite in sign, in the piezoelectric sheet charge arising from stress in the GaN channel layer.[18]

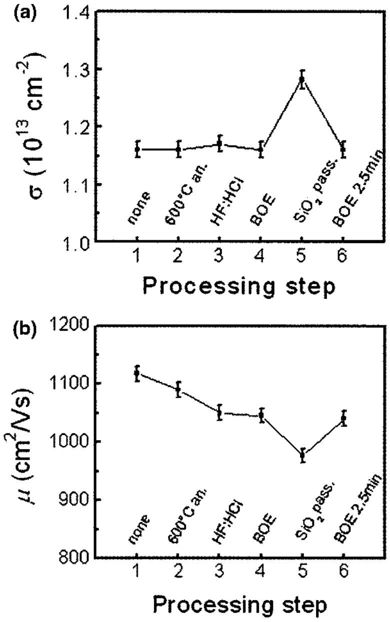

FIG. 2. (a) Sheet carrier concentration and (b) mobility derived from Hall measurements after annealing, surface processing treatments, SiO_2 deposition, and removal of the SiO_2 layer by wet etching for the doped-barrier structure shown in Fig. 1(a).

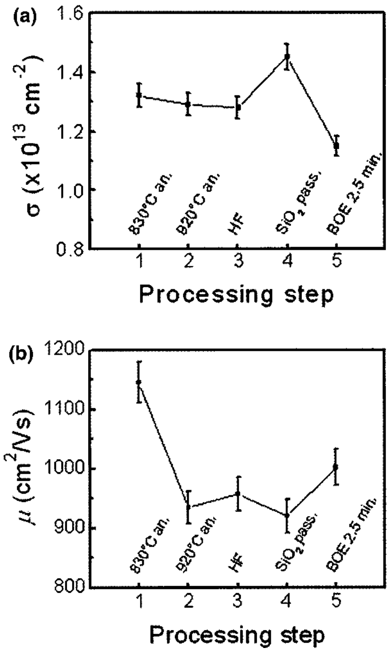

FIG. 3. (a) Sheet carrier concentration and (b) mobility derived from Hall measurements after annealing, surface processing treatments, SiO_2 deposition, and removal of the SiO_2 layer by wet etching for the undoped-barrier structure shown in Fig. 1(b).

The influence of the $Al_xGa_{1-x}N$ surface on the 2DEG sheet carrier concentration can be seen most easily from a simple electrostatic analysis. Figure 4 shows the conduction-band-edge profile and electrostatic charge distribution for an $Al_xGa_{1-x}N$/GaN HFET epitaxial layer structure with a SiO_2 passivation layer. Spontaneous and piezoelectric polarization effects lead to the existence of polarization-induced sheet charges at the $Al_xGa_{1-x}N$/GaN heterojunction interface, $\sigma_{\mathrm{pol,hj}}$, and at the $Al_xGa_{1-x}N/SiO_2$ interface, $\sigma_{\mathrm{pol,surf}}$. The former is due to the discontinuities in strain and spontaneous polarization at the $Al_xGa_{1-x}N$/GaN heterojunction interface,

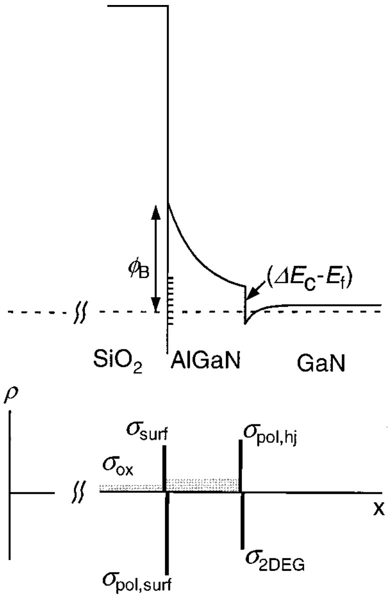

FIG. 4. Schematic diagrams of the conduction-band-edge profile and electrostatic charge distribution in an $Al_xGa_{1-x}N$/GaN HFET structure with SiO$_2$ passivation layer.

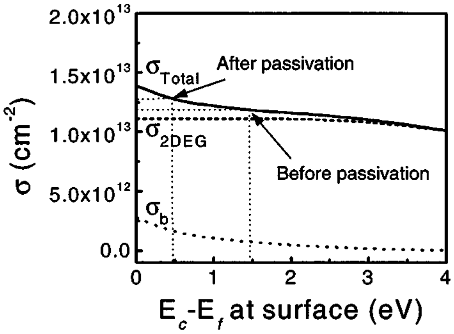

FIG. 5. Sheet carrier concentrations in the $Al_{0.25}Ga_{0.75}N$/GaN 2DEG (n_s) and the $Al_{0.25}Ga_{0.75}N$ barrier (n_b) along with their sum (n_{tot}) determined by numerical simulation as a function of $E_c - E_f$ at the $Al_{0.25}Ga_{0.75}N$ surface for the doped-barrier structure shown in Fig. 1(a). Measured carrier concentrations before and after deposition of the SiO$_2$ passivation layer, along with the corresponding values of $E_c - E_f$, are indicated.

and the latter to the piezoelectric and spontaneous polarization within the $Al_xGa_{1-x}N$ layer. In addition to these polarization-induced charge densities are those arising from donors in the $Al_xGa_{1-x}N$ layer (eN_d), charge within the SiO$_2$ layer (σ_{ox}), electrons in the 2DEG ($\sigma_{2DEG} \equiv en_s$), and electronic states at the $Al_xGa_{1-x}N$/SiO$_2$ interface (σ_{int}). In the absence of the SiO$_2$ passivation layer, states at the $Al_xGa_{1-x}N$ surface would lead to the existence of a surface charge σ_{surf}.

Following the analysis of Refs. 18 and 20, the charge density in the 2DEG is given by

$$\sigma_{2DEG} = \frac{\epsilon_b}{d}\left(\phi_b - \frac{\Delta E_c - E_f}{e}\right) - \frac{1}{2} eN_d d - \sigma_{pol,hj}, \tag{1}$$

where e is the electron charge, N_d and d are the dopant concentration within and thickness of the $Al_xGa_{1-x}N$ barrier layer, respectively, ϵ_b is the dielectric constant of the $Al_xGa_{1-x}N$ layer, ΔE_c is the $Al_xGa_{1-x}N$/GaN conduction-band offset, E_f is the Fermi energy at the $Al_xGa_{1-x}N$/GaN interface, and $e\phi_b$ is the energy difference between the Fermi level and $Al_xGa_{1-x}N$ conduction-band edge at the $Al_xGa_{1-x}N$/SiO$_2$ interface (or at the free $Al_xGa_{1-x}N$ surface in the absence of the SiO$_2$ passivation layer). From Eq. (1), we see that the only quantity upon which σ_{2DEG} depends that will be influenced by the presence of the SiO$_2$ passivation layer is ϕ_b; thus, any change in n_s induced by the presence of the SiO$_2$ layer should reflect a corresponding change in ϕ_b for the $Al_xGa_{1-x}N$/SiO$_2$ interface relative to that for the free $Al_xGa_{1-x}N$ surface.

These basic trends have been confirmed in detailed numerical simulations using a self-consistent one-dimensional Poisson solver.[21] In these simulations, the $Al_xGa_{1-x}N$ barrier thickness was assumed to be 245 Å (as determined from capacitance–voltage profiling for the undoped-barrier sample), and the background donor concentration in nominally undoped $Al_xGa_{1-x}N$ regions was assumed to be $2 \times 10^{18}\,\mathrm{cm}^{-3}$. Polarization charge densities at the $Al_xGa_{1-x}N$/GaN interface of $1.06 \times 10^{13}\,e/\mathrm{cm}^2$ and $1.36 \times 10^{13}\,e/\mathrm{cm}^2$ were assumed for Al concentrations of 25% and 30%, respectively. The background donor concentrations and polarization charge densities were chosen to yield a value of ϕ_b at the free $Al_xGa_{1-x}N$ surface consistent with measured sheet carrier concentrations and the experimental value of the $Al_xGa_{1-x}N$ free-surface barrier height reported by Ibbetson *et al.*[19]

Figures 5 and 6 show sheet carrier concentrations derived from these simulations as functions of ϕ_b for samples with doped and undoped $Al_xGa_{1-x}N$ barriers, respectively. Sheet carrier concentrations in the 2DEG and in the $Al_xGa_{1-x}N$ barrier, together with their sum, are plotted. The carrier concentrations obtained from the Hall measurements reported here are sums of the carrier concentrations in the 2DEG and $Al_xGa_{1-x}N$ barrier, and are also indicated in the figures for samples with and without SiO$_2$ passivation layers. As shown in the figures, the change in sheet carrier concentration induced by the presence of the SiO$_2$ passivation layer corresponds to a reduction in ϕ_b, upon deposition of the SiO$_2$ passivation layer, of approximately 1.0 V for the doped

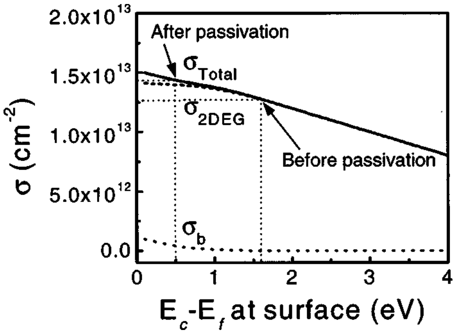

FIG. 6. Sheet carrier concentrations in the $Al_{0.30}Ga_{0.70}N$/GaN 2DEG (n_s) and the $Al_{0.30}Ga_{0.70}N$ barrier (n_b) along with their sum (n_{tot}) determined by numerical simulation as a function of $E_c - E_f$ at the $Al_{0.30}Ga_{0.70}N$ surface for the doped-barrier structure shown in Fig. 1(b). Measured carrier concentrations before and after deposition of the SiO$_2$ passivation layer, along with the corresponding values of $E_c - E_f$, are indicated.

$Al_{0.25}Ga_{0.75}N$ barrier, and of approximately 1.1 V for the undoped $Al_{0.30}Ga_{0.70}N$ barrier. From these observations we may conclude that the electronic density of states at the $Al_xGa_{1-x}N/SiO_2$ interface differs considerably from that of the free $Al_xGa_{1-x}N$ surface; the Fermi level at the $Al_xGa_{1-x}N/SiO_2$ interface is considerably closer to that expected for an unpinned surface, consistent with what one might expect on the basis of studies of GaN/SiO_2 interfaces that suggest the presence of relatively low densities of interface states.[22–25]

Our simulation results may also be used to assess the origins of the reduction in mobility induced by the presence of the SiO_2 passivation layer. Denoting the sheet carrier concentration and mobility in the 2DEG by n_s and μ_{2DEG}, respectively, and those in the $Al_xGa_{1-x}N$ barrier by n_b and μ_b, we estimate the measured mobility μ to be given by

$$\mu=(n_s\mu_{2DEG}+n_b\mu_b)/(n_s+n_b). \tag{2}$$

As shown in Figs. 5 and 6, the increases in carrier concentration induced by the presence of the SiO_2 passivation layer correspond partly to increased carrier concentrations in the $Al_xGa_{1-x}N$ barrier relative to those in the 2DEG. Since the mobility in the $Al_xGa_{1-x}N$ barrier is expected to be considerably lower than that in the 2DEG, a reduction in overall mobility upon deposition of the SiO_2 passivation layer is to be expected. From the data shown in Figs. 2(b) and 3(b) immediately prior to and following deposition of the SiO_2 passivation layer, we derive values of 1090 and 280 $cm^2/V\,s$ for μ_{2DEG} and μ_b, respectively, for the sample containing a doped $Al_{0.25}Ga_{0.75}N$ barrier, and values of 950 and 100 $cm^2/V\,s$ for μ_{2DEG} and μ_b, respectively, for the sample containing an undoped $Al_{0.30}Ga_{0.70}N$ barrier. The values derived for μ_{2DEG} are within expectations for $Al_xGa_{1-x}N/GaN$ HFET samples, and the values for μ_b are consistent with those derived from analysis of current-voltage characteristics in $Al_xGa_{1-x}N/GaN$ HFETs.[26]

The observed increase in carrier concentration following deposition of the SiO_2 passivation layer should lead to reductions in source and drain series resistance in an $Al_xGa_{1-x}N/GaN$ HFET device, resulting in an increase in transistor currents.[27] These expectations are consistent with studies in which an increase in saturated current density was reported following silicon nitride passivation of an $Al_xGa_{1-x}N/GaN$ HFET.[13] The reduction in ϕ_b deduced from our measurements indicates that the $Al_xGa_{1-x}N/SiO_2$ interface contains a significantly different electronic density of states compared to that present at the free $Al_xGa_{1-x}N$ surface, and studies of GaN/SiO_2 interfaces suggest the presence of a relatively low density of states at the nitride–SiO_2 interface.[22–25]

Studies of $Al_xGa_{1-x}N/GaN$ HFET structures have also been invoked to suggest that donor-like states at the $Al_xGa_{1-x}N$ surface with a density of $1.1\times10^{13}\,cm^{-2}$ or higher are present and become positively charged, thereby compensating much of the negative polarization charge at the $Al_xGa_{1-x}N$ surface and providing carriers to the 2DEG at the $Al_xGa_{1-x}N/GaN$ interface.[19] Should the presence of SiO_2 silicon nitride, or other dielectric passivation layers lead to a reduction in surface-state density, the mechanisms by which the polarization charge at the AlGaN surface is compensated and by which carriers are provided to the 2DEG would remain to be elucidated. Charges in the passivation layer, as indicated schematically in Fig. 4, are one possibility.

IV. CONCLUSIONS

We have performed detailed studies of the influence of a variety of annealing procedures, surface processing treatments, and surface passivation layers on carrier concentrations and transport properties in $Al_xGa_{1-x}N/GaN$ HFET epitaxial layer structures. In previous studies, silicon nitride passivation layers have been found to lead to increased dc current density and improved rf power output in $Al_xGa_{1-x}N/GaN$ HFET's,[13] and SiO_2 surface passivation was found to reduce leakage current in III–V nitride Schottky diodes.[14] In addition, there is growing interest in the use of SiO_2 as a gate insulator in III–V nitride HFETs.[15,28] The current studies were motivated by a desire to assess the influence of surface processing and of surface passivation layers on the electronic properties of the $Al_xGa_{1-x}N$ surface and, by extension, the properties of the 2DEG in an $Al_xGa_{1-x}N/GaN$ HFET structure. Our studies have shown that surface chemical treatments have little effect on 2DEG carrier concentration and produce at most a slight degradation in mobility. However, deposition of a SiO_2 layer by PECVD induces a significant increase in carrier concentration and decrease in mobility that is largely reversed upon removal of the SiO_2 layer by wet etching. The observed increases in carrier concentration and reductions in mobility are quantitatively consistent with a shift in the Fermi level at the $Al_xGa_{1-x}N$ surface of approximately 1 eV towards the conduction-band edge in the presence of the SiO_2 layer compared to its position for the free $Al_xGa_{1-x}N$ surface for Al concentrations of 25%–30%. These results indicate that the electronic density of states at the $Al_xGa_{1-x}N$ surface is altered significantly, and possibly reduced, in the presence of the SiO_2 passivation layer. In the latter case, alternate mechanisms for compensation of polarization charge at the AlGaN surface and for providing carriers to the 2DEG might need to be invoked.

ACKNOWLEDGMENT

Part of this work was supported by BMDO (Dr. Kepi Wu, DASG60-00-1-0006).

[1] Y. F. Wu, B. P. Keller, P. Fini, S. Keller, T. J. Jenkins, L. T. Kehias, S. P. Denbaars, and U. K. Mishra, IEEE Electron Device Lett. **19**, 50 (1998).
[2] S. T. Sheppard, K. Doverspike, W. L. Pribble, S. T. Allen, J. W. Palmour, L. T. Kehias, and T. J. Jenkins, IEEE Electron Device Lett. **20**, 161 (1999).
[3] G. J. Sullivan, M. Y. Chen, J. A. Higgins, J. W. Yang, Q. Chen, R. L. Pierson, and B. T. McDermott, IEEE Electron Device Lett. **19**, 198 (1998).
[4] N. X. Nguyen, M. Micovic, W. S. Wong, P. Hashimoto, L. M. McCray, P. Janke, and C. Nguyen, Electron. Lett. **36**, 468 (2000).
[5] Q. Chen, R. Gaska, M. Asif Khan, M. S. Shur, A. Ping, I. Adesida, J. Burm, W. J. Schaff, and L. F. Eastman, Electron. Lett. **33**, 637 (1997).
[6] M. A. Khan, M. S. Shur, Q. C. Chen, and J. N. Kuznia, Electron. Lett. **30**, 2175 (1994).
[7] P. B. Klein, J. A. Freitas, Jr., S. C. Binari, and A. E. Wickenden, Appl. Phys. Lett. **75**, 4016 (1999).

[8] S. C. Binari, W. Kruppa, H. B. Dietrich, G. Kelner, A. E. Wickenden, and J. A. Freitas Jr., Solid-State Electron. **41**, 1549 (1997).

[9] S. C. Binari, IEEE Intel. Microwave Symp. Digest **3.4**, 1081 (1999).

[10] S. Trassaert, B. Boudart, C. Gaquiere, D. Theron, Y. Crosnier, F. Huet, and M. A. Poisson, Electron. Lett. **35**, 1386 (1999).

[11] E. Kohn, I. Daumiller, P. Schmid, N. X. Nguyen, and C. N. Nguyen, Electron. Lett. **35**, 1022 (1999).

[12] X. Z. Dang, P. M. Asbeck, E. T. Yu, K. S. Boutros, and J. M. Redwing, Mater. Res. Soc. Symp. Proc. **622**, T.28.1 (2000).

[13] B. M. Green, K. K. Chu, E. M. Chumbes, J. A. Smart, J. R. Shealy, and L. F. Eastman, IEEE Electron Device Lett. **21**, 268 (2000).

[14] V. Adivarahan, G. Simin, J. W. Yang, A. Lunev, M. Asif Khan, N. Pala, M. Shur, and R. Gaska, Appl. Phys. Lett. **77**, 863 (2000).

[15] M. Asif Khan, X. Hu, G. Sumin, A. Lunev, J. Yang, R. Gaska, and M. S. Shur, IEEE Electron Device Lett. **21**, 63 (2000).

[16] F. Ren *et al.*, Solid-State Electron. **43**, 1817 (1999).

[17] M. Hong *et al.*, J. Vac. Sci. Technol. B **18**, 1453 (2000).

[18] E. T. Yu, G. J. Sullivan, P. M. Asbeck, C. D. Wang, D. Qiao, and S. S. Lau, Appl. Phys. Lett. **71**, 2794 (1997).

[19] J. P. Ibbetson, P. T. Fini, K. D. Ness, S. P. DenBaars, J. S. Speck, and U. K. Mishra, Appl. Phys. Lett. **77**, 250 (2000).

[20] E. T. Yu, X. Z. Dang, L. S. Yu, D. Qiao, P. M. Asbeck, S. S. Lau, G. J. Sullivan, K. S. Boutros, and J. M. Redwing, Appl. Phys. Lett. **73**, 1880 (1998).

[21] G. L. Snider, computer program *1D Poisson/Schrödinger: A Band Diagram Calculator*, University of Notre Dame, 1995.

[22] S. Arulkumaran, T. Egawa, H. Ishikawa, T. Jimbo, and M. Umeno, Appl. Phys. Lett. **73**, 809 (1998).

[23] H. C. Casey, Jr., G. G. Fountain, R. G. Alley, B. P. Keller, and S. P. DenBaars, Appl. Phys. Lett. **68**, 1850 (1996).

[24] M. Sawada, T. Sawada, Y. Yamagata, K. Imai, H. Kimura, M. Yoshino, K. Iizuka, and H. Tomozama, J. Cryst. Growth **189/190**, 706 (1998).

[25] R. Therrien, G. Lucovshi, and R. F. Davis, Phys. Status Solidi A **176**, 793 (1999).

[26] X. Z. Dang, P. M. Asbeck, E. T. Yu, G. J. Sullivan, M. Y. Chen, B. T. McDermott, K. S. Boutros, and J. M. Redwing, Appl. Phys. Lett. **74**, 3890 (1999).

[27] S. M. Sze, *Modern Semiconductor Device Physics* (Wiley, New York, 1998), Chap. 2.

[28] N. Pala, R. Gaska, S. Rumyantsev, M. S. Shur, M. Asif Khan, X. Hu, G. Simin, and J. Yang, Electron. Lett. **36**, 268 (2000).